Fluid demixing in colloid–polymer mixtures: Influence of polymer interactions

Matthias Schmidt
Institut für Theoretische Physik, Heinrich-Heine Universität Düsseldorf, Universitätsstraße 1, D-40225 Düsseldorf, Germany

Alan R. Denton
Department of Physics, North Dakota State University, Fargo, North Dakota 58105-5566

Joseph M. Brader
The James Franck Institute, University of Chicago, Chicago, Illinois 60637

(Received 29 July 2002; accepted 17 October 2002)

We consider a binary mixture of hard colloidal spheres and nonadsorbing polymer coils. The polymers are regarded as effective spheres that interact with one another via a repulsive step-function pair potential and with colloids solely via excluded volume. The system is treated with a geometry-based density functional theory based on the exact zero-dimensional limit of the model. For bulk fluid phases, we calculate demixing binodals and find that with increasing strength of polymer–polymer interaction the coexisting colloidal liquid (vapor) phase becomes more concentrated (dilute) in polymer. In contrast to a simple mean-fieldlike perturbative density functional, our approach yields good agreement with an experimental demixing phase diagram. [DOI: 10.1063/1.1528191]

I. INTRODUCTION

Colloid–polymer mixtures are experimentally accessible, well-characterized systems, that serve as models for studying emergence of structure in condensed matter. In particular, phase transitions between colloidal vapor, liquid, and crystalline phases have attracted much experimental and theoretical interest. For mixtures of colloids and nonadsorbing polymer, the Asakura–Oosawa (AO) model[1,2] treats the polymer chains as effective spheres that are mutually ideal (noninteracting) but that have excluded-volume interactions with the colloids. Within the AO model, perturbation theory[3] and free-volume theory[4] predict bulk fluid demixing, the latter theory qualitatively describing experimental trends of the phase behavior.[5,6]

Recent work has been devoted to integrating out polymer degrees of freedom to obtain an effective (many-body) Hamiltonian for the colloids.[7] A pairwise approximation to the effective Hamiltonian can then be input to standard bulk perturbation theory in order to calculate thermodynamic and structural properties.[7] This principle approach was also used for investigation of interfacial properties[8,9] in the framework of density-functional theory (DFT).[10]

An alternative approach is to explicitly treat the full binary mixture and hence effective many-body colloidal interactions. Following previous work on hard sphere mixtures,[11–15] a DFT approach to the AO model was recently proposed.[16,17] The bulk fluid free energy, and hence the fluid–fluid demixing phase diagram, that arise from this DFT are identical to the predictions of free volume theory.[4] However, as the theory is constructed to deal with inhomogeneous systems, it also can be applied to (entropic) wetting at a hard wall and layering phenomena in the interface between demixed fluids.[18]

All of these approaches neglect direct polymer–polymer interactions, an assumption that is most valid at the theta temperature, where the second virial coefficient of the monomer–monomer interaction vanishes. In order to treat interactions between polymers, Warren *et al.*[19] proposed a perturbation theory around the AO model as a reference system (which, again, is described with free-volume theory). A more microscopic picture that works on the segment level of the polymers is provided by the macromolecular approach of Fuchs and co-workers.[20,21] In their theory, interactions between segments (and hence polymers) are intrinsically built in. However, both approaches seem to be limited primarily to *bulk* considerations.

Although a description on the segment level is desirable, we note that for pure polymer solutions, recent studies have suggested a ''soft colloid'' picture.[22] In this picture, upon averaging over the monomer degrees of freedom, effective polymer interactions can be well represented by a Gaussian pair potential. Such penetrable potentials have been shown to be well described by a simple mean-fieldlike density functional, which in bulk is equivalent to the random phase approximation (RPA).[22] In the same spirit, a recent study examined the *binary* Gaussian core mixture in inhomogeneous situations.[23,24] In the context of colloid–polymer interactions, structural correlation functions were obtained from the Percus–Yevick theory applied to the AO model and also a (Gaussian) repulsion between polymers was taken into account.[25]

In the present work, we aim at a DFT for a more realistic description of colloid–polymer mixtures than provided by the AO model, one that takes polymer–polymer interactions into account. Specifically, we consider a model in which the polymers, although still treated as effective spheres, interact

via a repulsive step-function pair potential. This model bridges recent studies by interpolating between the AO model for ideal polymers and the binary hard-sphere (HS) mixture. Note that while the AO model system displays stable fluid–fluid coexistence,[3,4,7] binary HS mixtures do not, as freezing preempts fluid demixing.[26]

In Sec. II, the model mixture of colloids and interacting polymers is defined. In Sec. III, we develop the nonperturbative geometry-based DFT. The explicit construction of the functional is guided by the exact solution of the model in the special zero-dimensional case. For comparison, we also discuss two mean-fieldlike perturbative theories. In Sec. IV, we derive the bulk free energy, which allows us to calculate phase behavior. We conclude in Sec. V.

II. THE MODEL

We consider a binary mixture of hard colloidal spheres (species C) of radius R_C and polymer coils (species P) with radius of gyration R_P. The colloid–colloid pair interaction potential as a function of the center–center interparticle distance, r, is $V(r)=\infty$, if $r<2R_C$, and zero otherwise. We assume that the polymer–colloid interaction is also hard: $V_{CP}(r)=\infty$, if $r<R_C+R_P$, and zero otherwise. The interactions between polymers are represented by a step-function pair potential: $V_{PP}(r)=\epsilon$, if $r<2R_P$, and zero otherwise. Apart from trivial kinetic energy terms and external potentials, the resulting Hamiltonian is

$$H(\{\mathbf{R}_i\},\{\mathbf{r}_j\})=\sum_{i<j}^{N_C} V_{CC}(|\mathbf{R}_i-\mathbf{R}_j|)+\sum_{i}^{N_C}\sum_{j}^{N_P} V_{CP}(|\mathbf{R}_i-\mathbf{r}_j|)+\sum_{i<j}^{N_P} V_{PP}(|\mathbf{r}_i-\mathbf{r}_j|), \tag{1}$$

where $\{\mathbf{R}_i\}$ denotes colloid and $\{\mathbf{r}_j\}$ polymer coordinates. Note that in the limit $\epsilon/k_BT\to 0$ we recover the AO model, and for $\epsilon/k_BT\to\infty$ binary hard spheres. Although in Ref. 19 $V_{PP}(r)$ is assumed to have a range of R_P, our (longer-ranged) choice is more consistent with the effective (Gaussian) potentials of Louis *et al.*,[22] which extend out even beyond $2R_P$. We do not use the Gaussian potential as our aim is at a minimal model that displays the essential features.

As bulk thermodynamic parameters, we use the packing fractions $\eta_i=4\pi R_i^3\rho_i/3$, $i=C,P$, where ρ_i is the number density of species i. The control parameters are the size ratio, $q=R_P/R_C$, of colloid and polymer radii and the reduced strength, $\epsilon/(k_BT)$, of polymer–polymer interactions, where k_B is the Boltzmann constant and T absolute temperature.

III. THEORY

A. Zero-dimensional limit

In the original context of hard spheres,[14] it was shown that an idealized zero-dimensional (0D) limit can motivate the construction of density functionals for 3D systems. The benefit of zero dimensions is that the partition sum can be calculated exactly, as the configurational integral over the spatial degrees of freedom is trivial. Choosing an explicit (approximate) form for the free energy functional, one imposes that it correctly recovers the 0D properties, when applied to an appropriate (δ-functionlike) density profile. This constraint has guided the development of DFTs for models such as penetrable spheres[27] and the AO model.[16,17]

Let us consider the current model in the 0D limit, in which particle centers are confined to a volume v_{0D} whose dimensions are smaller than all relevant length scales in the system. The microstates accessible in that limit are completely specified by the occupation numbers of particles of both species. Each microstate is assigned a statistical weight according to the grand ensemble. In general, the grand partition sum for a binary mixture is

$$\Xi=\sum_{N_P=0}^{\infty}\frac{z_P^{N_P}}{N_P!}\sum_{N_C=0}^{\infty}\frac{z_C^{N_C}}{N_C!}\exp(-\beta V_{\text{total}}), \tag{2}$$

where the (reduced) fugacities are $z_i=(v_{0D}/\Lambda_i^3)\exp(\beta\mu_i)$, Λ_i is the thermal wavelength, μ_i is the chemical potential of species i, $\beta=(k_BT)^{-1}$, and V_{total} is the total potential energy in the situation where all particles have vanishing separation. Note that for hard-core interactions, the Boltzmann factor vanishes for forbidden configurations, which practically limits the upper bounds in the summations in Eq. (2). For the present case, where V_{CC} and V_{CP} are hard-body interactions, we obtain

$$\Xi=z_C+\sum_{N_P=0}^{\infty}\frac{z_P^{N_P}}{N_P!}\exp[-\beta\epsilon N_P(N_P-1)/2], \tag{3}$$

where the N_P dependence in the Boltzmann factor stems from combinatorial counting of pairs of polymers. Clearly, for $z_C=0$, we recover the limit of one-component penetrable spheres;[27] for $\beta\epsilon=0$, Eq. (3) reduces to the AO result,[16,17] $\Xi=z_C+\exp(z_P)$. In order to obtain the Helmholtz free energy, a Legendre transform is to be performed, and the dependence on the fugacities is to be replaced with dependence on the mean numbers of particles, $\eta_i=z_i\partial\ln\Xi/\partial z_i$. Taking the particle volume of species i as the reference volume, η_i is also the 0D packing fraction of species i. Subtracting the ideal contribution, one calculates the excess free energy, $\beta F_{0D}=-\ln\Xi+\Sigma_{i=C,P}\eta_i\ln(z_i)-\Sigma_{i=C,P}\eta_i[\ln(\eta_i)-1]$. In the present case (as for pure penetrable spheres), this cannot be achieved analytically. As we are interested in the case of small ϵ (close to the AO behavior), we perform an expansion in powers of $\beta\epsilon$, and obtain

$$\beta F_{0D}=(1-\eta_C-\eta_P)\ln(1-\eta_C)+\eta_C+\frac{\beta\epsilon}{2}\frac{\eta_P^2}{1-\eta_C}, \tag{4}$$

which is exact up to lowest (linear) order in $\beta\epsilon$. In the limit $\beta\epsilon\to 0$, we recover the AO result,[16,17] which is $\beta F_{0D,AO}=(1-\eta_C-\eta_P)\ln(1-\eta_C)+\eta_C$. In the absence of colloids, $\eta_C\to 0$, we obtain a mean-fieldlike expression, $F_{0D,MF}=\epsilon\eta_P^2/2$.

Some terms of higher than first order can be obtained analytically. We write the free energy as $F_{0D}+\Delta F_{0D}$, where F_{0D} is the linear contribution given by Eq. (4) and ΔF_{0D} up to cubic order in $\beta\epsilon$ is obtained as

$$\beta\Delta F_{0D}=-\frac{\eta_P^2(\beta\epsilon)^2}{4(1-\eta_C)}+\left[\frac{\eta_P^2}{1-\eta_C}+\frac{2\eta_P^3}{(1-\eta_C)^2}\right]\frac{(\beta\epsilon)^3}{12}. \tag{5}$$

In the case of large $\beta\epsilon$, the 0D free energy has to be calculated numerically, which is an easy task.

B. Geometry-based density functional

Returning to three dimensions, the total Helmholtz free energy of an inhomogeneous system may be written as $F=F_{\rm id}+F_{\rm exc}$, where $F_{\rm id}=\Sigma_{i=C,P}\int d\mathbf{r}\rho_i(\mathbf{r})\{\ln[\rho_i(\mathbf{r})\Lambda_i^3]-1\}$ is the ideal-gas free energy functional (for two species), and $F_{\rm exc}$ is the excess contribution arising from interactions between particles. Following previous work on mixtures,[11–13,16,17] we express the Helmholtz excess free energy as a functional of colloid and polymer density fields as a spatial integral

$$F_{\rm exc}[\rho_C(\mathbf{r}),\rho_P(\mathbf{r})]=k_BT\int d^3x\Phi(\{n_\nu^C(\mathbf{x})\},\{n_\gamma^P(\mathbf{x})\}), \tag{6}$$

where the weighted densities

$$n_\nu^i(\mathbf{x})=\int d^3r\rho_i(\mathbf{r})w_\nu^i(\mathbf{x}-\mathbf{r}),\quad i=C,P \tag{7}$$

are defined as convolutions of weight functions, w_ν^i, with the actual density profiles, and ν denotes the type of weight function.

In previous work on HS,[11] Φ is a function of species-independent weighted densities. Here we use the generalized form introduced in Ref. 16, where Φ is a function of species-dependent weighted densities. This form was shown to be necessary to capture the distinct properties of colloids and polymers. The weight functions w_ν^i are independent of the density profiles and are given by

$$w_3^i(\mathbf{r})=\theta(R_i-r),\quad w_2^i(\mathbf{r})=\delta(R_i-r), \tag{8}$$

$$\mathbf{w}_{\rm v2}^i(\mathbf{r})=w_2^i(\mathbf{r})\mathbf{r}/r,\quad \hat{\mathbf{w}}_{\rm m2}^i(\mathbf{r})=w_2^i(\mathbf{r})[\mathbf{rr}/r^2-\hat{\mathbf{1}}/3], \tag{9}$$

where $r=|\mathbf{r}|$, $\theta(r)$ is the step function, $\delta(r)$ is the Dirac distribution, and $\hat{\mathbf{1}}$ is the identity matrix. Further, linearly dependent, weights are $w_1^i(\mathbf{r})=w_2^i(\mathbf{r})/(4\pi R_i)$, $\mathbf{w}_{\rm v1}^i(\mathbf{r})=\mathbf{w}_{\rm v2}^i(\mathbf{r})/(4\pi R_i)$, $w_0^i(\mathbf{r})=w_1^i(\mathbf{r})/R_i$. The weight functions are quantities with dimension $(\text{length})^{\nu-3}$. They differ in their tensorial rank: w_0^i, w_1^i, w_2^i, w_3^i are scalars; $\mathbf{w}_{\rm v1}^i$, $\mathbf{w}_{\rm v2}^i$ are vectors (subscript v); and $\hat{\mathbf{w}}_{\rm m2}^i$ is a (traceless) matrix (subscript m). The scalar and vectorial weights are borrowed from Ref. 11, whereas the tensor weight is equivalent to the formulation in Ref. 15.

The free energy density is composed of three parts,

$$\Phi=\Phi_1+\Phi_2+\Phi_3, \tag{10}$$

which are defined as

$$\Phi_1=\sum_{i=C,P}n_0^i\varphi_i(n_3^C,n_3^P), \tag{11}$$

$$\Phi_2=\sum_{i,j=C,P}(n_1^in_2^j-\mathbf{n}_{\rm v1}^i\cdot\mathbf{n}_{\rm v2}^j)\varphi_{ij}(n_3^C,n_3^P), \tag{12}$$

$$\Phi_3=\frac{1}{8\pi}\sum_{i,j,k=C,P}\left(\frac{1}{3}n_2^in_2^jn_2^k-n_2^i\mathbf{n}_{\rm v2}^j\cdot\mathbf{n}_{\rm v2}^k+\frac{3}{2}[\mathbf{n}_{\rm v2}^i\hat{\mathbf{n}}_{\rm m2}{}^j\mathbf{n}_{\rm v2}^k-{\rm tr}(\hat{\mathbf{n}}_{\rm m2}{}^i\hat{\mathbf{n}}_{\rm m2}{}^j\hat{\mathbf{n}}_{\rm m2}{}^k)]\right)\times\varphi_{ijk}(n_3^C,n_3^P), \tag{13}$$

where tr denotes the trace, and derivatives of the 0D excess free energy [Eq. (4)] are

$$\varphi_{i\cdots k}(\eta_C,\eta_P)\equiv\frac{\partial^m}{\partial\eta_i\cdots\partial\eta_k}F_{0D}(\eta_C,\eta_P). \tag{14}$$

In the absence of polymer, Φ_1 and Φ_2 are treated as in Ref. 11 and Φ_3 as in Ref. 15. Equations (11)–(13) are generalizations of expressions in Refs. 11 and 15 that include summations over species.[16,17]

C. Perturbative density functional

It is instructive to relate the above approach to a perturbative treatment, where the AO model is used as a reference system, and the polymer–polymer interactions are regarded as a perturbation. Apparently, perturbed and reference systems are very similar. Aside from sharing the same V_{CC}, the cross interactions V_{CP} are the same (namely hard-core interactions). Only the remaining polymer–polymer interaction differs (and vanishes in the reference system). The reference system may be well described by the AO functional,[16,17] which is recovered by using $F_{0D}=(1-\eta_C-\eta_P)\ln(1-\eta_C)+\eta_C$ as a generator in the above geometrical recipe. What remains to be treated is the perturbative contribution to the free energy due to polymer–polymer interactions. To obtain that, a minimal requirement is that the pure polymer system (free of colloids) is described reasonably. As was recently discovered[28] for penetrable interactions, this is the case for a mean-field (excess) functional

$$F_{\rm MF}[\rho_P(\mathbf{r})]=\tfrac{1}{2}\int d\mathbf{r}\,d\mathbf{r}'\rho_P(\mathbf{r})V_{PP}(|\mathbf{r}-\mathbf{r}'|)\rho_P(\mathbf{r}'). \tag{15}$$

This DFT was utilized to investigate Gaussian core particles adsorbed at a hard wall.[28] The generalization of Eq. (15) to binary mixtures was used in Ref. 23 to study interfacial properties[23] and wetting[24] of the binary Gaussian core model. Note that in bulk Eq. (15) is equivalent to using the RPA, which is a reasonable approximation for penetrable interactions.[29,30]

It might at first appear that $F'=F_{\rm AO}+F_{\rm MF}$ would give a good description of the excess free energy of the mixture, as the hard-body interactions between polymers and colloids are already accounted for in $F_{\rm AO}$. Hence the perturbative contribution depends *solely on the polymer density profile.* This reasoning is independent of the precise model under consideration, and should hold also for soft repulsive interactions. For the present model, we can show, in contrast, that F' is (apart from trivial limits) never a good approximation to treat the mixture, and nonsensical trends in phase behavior

arise (see Sec. IV C). We expect similar failings when applying this approach to other models consisting of mixtures of hard-core and penetrable particles.

Within our framework, F' can be derived from $F_{0D} = F_{0D}^{AO} + \epsilon \eta_P^2/2$ and applying the recipe outlined in Sec. III B. By comparing with the exact linear-order result [Eq. (4)], $F_{0D} = F_{0D}^{AO} + \frac{1}{2}\epsilon \eta_P^2/(1-\eta_C)$, one immediately observes that already the linear term in η_C differs. This discrepancy persists throughout the construction of the DFT, and hence F' displays a similar failing. The predictions of phase behavior from this approach are shown at the end of Sec. IV C below.

Evidently, the mean-field functional neglects exclusion of polymer from the volume occupied by the colloid. In contrast, the geometry-based functional naturally accounts for excluded volume: A given polymer interacts with polymer in the available volume whose density is higher than the density of polymer in the system.

D. Perturbative bulk theory

Warren *et al.*[19] proposed a perturbative approach for the free energy of bulk colloid–polymer mixtures in which polymers interact with a penetrable repulsive interaction $V_{PP}(r)$. This can be viewed as a perturbative treatment where in the reference system $V_{PP}(r)=0$, and $V_{PP}(r)$ is regarded as the perturbation. As input, the bulk void–void correlation function[31] of the pure hard sphere system is required, and Ref. 19 proposes an empirical analytical form that interpolates between the known limits of vanishingly and infinitely separated polymers. In the following, we rederive this theory in a general framework. This will allow us to relate the approach of Warren *et al.* to the oversimplistic bulk theory that arises from the perturbative DFT. Moreover, we can quantitatively compare this approach against the bulk predictions of the geometry-based DFT.

We consider the fully interacting binary mixture with fixed colloid particle number N_C and polymer fugacity z_P. The semigrand partition function is given by

$$\Xi_{\text{semi}} = \text{Tr}_C e^{-\beta H_{CC}} \left[\sum_{N_P=0}^{\infty} \frac{z_P^{N_P}}{N_P!} \int d\mathbf{r}^{N_P} e^{-\beta(H_{CP}+\lambda H_{PP})} \right], \tag{16}$$

where λ is a charging parameter which is equal to unity in the fully interacting system, and the canonical trace over colloid coordinates is

$$\text{Tr}_C = \frac{1}{\Lambda_C^{3N_C} N_C!} \int d\mathbf{R}^{N_C}. \tag{17}$$

By expanding the integrand in Eq. (16) in a Taylor series about $\lambda=0$, we obtain a perturbation theory

$$\beta\Omega_{\text{semi}} = \beta\Omega_{\text{semi},0} + \int_0^1 d\lambda \left(\frac{\partial \beta\Omega_{\text{semi}}}{\partial \lambda} \right) \approx \beta\Omega_{\text{semi},0} + \left(\frac{\partial \beta\Omega_{\text{semi}}}{\partial \lambda} \right)_0, \tag{18}$$

where $\beta\Omega_{\text{semi}} = -\ln \Xi_{\text{semi}}$. The first term on the right is the semigrand free energy of the AO model, given by

$$\beta\Omega_{\text{semi},0} = -\ln\left(\text{Tr}_C e^{-\beta H_{CC}} \sum_{N_P=0}^{\infty} \frac{z_P^{N_P}}{N_P!} \int d\mathbf{r}^{N_P} e^{-\beta H_{CP}} \right) \tag{19}$$

$$= -\ln\left(\text{Tr}_C e^{-\beta H_{CC}} \sum_{N_P=0}^{\infty} \frac{[z_P V \alpha(\{\mathbf{R}^{N_C}\})]^{N_P}}{N_P!} \right) \tag{20}$$

$$= -\ln\{\text{Tr}_C e^{-\beta H_{CC}} \exp[z_P V \alpha(\{\mathbf{R}^{N_C}\})]\}, \tag{21}$$

where $\alpha(\{\mathbf{R}^{N_C}\})$ is the ratio of the free volume of a single polymer sphere, in the presence of the colloids, to the system volume, V. By replacing the exact $\alpha(\{\mathbf{R}^{N_C}\})$, which depends on all coordinates of the colloids, by its average for hard spheres, $\Omega_{\text{semi},0}$ becomes identical to the result from the free-volume theory of Lekkerkerker *et al.*[4] The second term on the right side of Eq. (18) is given by

$$\left(\frac{\partial \beta\Omega_{\text{semi}}}{\partial \lambda} \right)_0 = \Xi_{\text{semi},0}^{-1} \text{Tr}_C e^{-\beta H_{CC}} \sum_{N_P=0}^{\infty} \frac{z_P^{N_P}}{N_P!} \int d\mathbf{r}^{N_P} \times \sum_{i<j} \beta V_{PP}(|\mathbf{r}-\mathbf{r}'|) e^{-\beta H_{CP}} \tag{22}$$

$$= \Xi_{\text{semi},0}^{-1} \text{Tr}_C e^{-\beta H_{CC}} \sum_{N_P=0}^{\infty} \frac{z_P^{N_P}}{N_P!} \times \int d\mathbf{r}^{N_P-2} \frac{N_P}{2}(N_P-1)\alpha(\{\mathbf{R}^{N_C}\})^{N_P-2} \times \int d\mathbf{r} \int d\mathbf{r}' \beta V_{PP} \times (|\mathbf{r}-\mathbf{r}'|)\alpha(\mathbf{r};\{\mathbf{R}^{N_C}\})\alpha(\mathbf{r}';\{\mathbf{R}^{N_C}\}) \tag{23}$$

$$= \Xi_{\text{semi},0}^{-1} \text{Tr}_C e^{-\beta H_{CC}} \int d\mathbf{r} \int d\mathbf{r}' \beta V_{PP} \times (|\mathbf{r}-\mathbf{r}'|)\alpha(\mathbf{r};\{\mathbf{R}^{N_C}\})\alpha(\mathbf{r}';\{\mathbf{R}^{N_C}\}) \times \frac{z_P^2}{2} \sum_{N_P=0}^{\infty} \frac{[z_P V \alpha(\{\mathbf{R}^{N_C}\})]^{N_P-2}}{(N_P-2)!}, \tag{24}$$

where $\Xi_{\text{semi},0}$ is the term inside the logarithm in Eq. (21). The final result is thus

$$\left(\frac{\partial \beta\Omega_{\text{semi}}}{\partial \lambda} \right)_0 = \Xi_{\text{semi},0}^{-1} \text{Tr}_C e^{-\beta H_{CC}} \exp[z_P V \alpha(\{\mathbf{R}^{N_C}\})] \times \frac{z_P^2}{2} \int d\mathbf{r} \int d\mathbf{r}' \beta V_{PP}(|\mathbf{r}-\mathbf{r}'|) \times \alpha(\mathbf{r};\{\mathbf{R}^{N_C}\})\alpha(\mathbf{r}';\{\mathbf{R}^{N_C}\}). \tag{25}$$

Equations (21) and (25) give the exact free energy to linear order in $\beta V_{PP}(r)$. We now proceed by making the mean-field approximations and replacing quantities by their average values in the unperturbed (AO) system

$$\alpha(\{\mathbf{R}^{N_C}\}) \to \alpha(\eta_C, z_P), \tag{26}$$

$$\alpha(\mathbf{r};\{\mathbf{R}^{N_C}\})\alpha(\mathbf{r}';\{\mathbf{R}^{N_C}\}) \to g_{vv}(|\mathbf{r}-\mathbf{r}'|;\eta_C,z_P), \tag{27}$$

where $\alpha(\eta_C, z_P)$ is the exact free volume fraction for the AO model (noninteracting polymers) and $g_{vv}(|\mathbf{r}-\mathbf{r}'|;\eta_C,z_P) \equiv \langle \alpha(\mathbf{r};\{\mathbf{R}^{N_C}\})\alpha(\mathbf{r}';\{\mathbf{R}^{N_C}\})\rangle_{\mathrm{AO}}$ is the void–void correlation function of the AO model. The voids are the spaces between the colloids that can be occupied by the polymer. Insertion of Eq. (26) into Eq. (21) clearly yields the exact AO free energy. The final result is thus

$$\beta\Omega_{\mathrm{semi}} = \beta\Omega_{\mathrm{semi,AO}} + \frac{z_P^2}{2} V \int d\mathbf{r}\ \beta V_{PP}(r) \times g_{vv}(|\mathbf{r}-\mathbf{r}'|;\eta_C,z_P). \tag{28}$$

If we now further approximate the relevant quantities by their HS values, $\alpha(\eta_C,z_P) \to \alpha(\eta_C) \equiv \alpha(\eta_C, z_P=0)$ and $g_{vv}(|\mathbf{r}-\mathbf{r}'|;\eta_C,z_P) \to g_{vv}^{\mathrm{HS}}(|\mathbf{r}-\mathbf{r}'|;\eta_C) \equiv g_{vv}(|\mathbf{r}-\mathbf{r}'|;\eta_C,z_P=0)$, then the first term reduces to the free-volume theory of Lekkerkerker *et al.* and we obtain

$$\beta\Omega_{\mathrm{semi}} = \beta F_{\mathrm{HS}} - z_P\alpha(\eta_C)V + \frac{z_P^2}{2} V \int d\mathbf{r}\ \beta V_{PP}(r) \times g_{vv}^{\mathrm{HS}}(|\mathbf{r}-\mathbf{r}'|;\eta_C), \tag{29}$$

where F_{HS} is the Helmholtz free energy of pure HS. We give the explicit (approximative) expression for $\alpha(\eta_C)$ below in Sec. IV A. The original result of Warren *et al.* for the semigrand free energy, Eq. (27) in Ref. 19, is identical to Eq. (29), if $\beta V_{PP}(r)$ in (29) is replaced by its corresponding Mayer function, $1-\exp[-\beta V_{PP}(r)]$. The difference arises from the fact that in the original version a virial expansion in polymer density is performed, while we apply thermodynamic perturbation theory. However, for small $\beta\epsilon$ the differences are negligible.

An equivalent perturbation theory can be derived directly in the canonical ensemble. The result for the canonical excess free energy is

$$\frac{\beta F_{\mathrm{exc}}^{\mathrm{pert}}(\rho_C,\rho_P)}{V} = \beta\phi_{\mathrm{HS}}(\rho_C) - \rho_P \ln\alpha(\rho_C) + \frac{\beta}{2}\left(\frac{\rho_P}{\alpha(\rho_C)}\right)^2 \int \mathrm{d}\mathbf{r} V_{PP}(r) \times g_{vv}^{\mathrm{HS}}(|\mathbf{r}-\mathbf{r}'|;\rho_C), \tag{30}$$

where $\phi_{\mathrm{HS}}(\rho_C)$ is the excess free energy per unit volume of pure HS. While the same level of approximation is employed in both derivations, Eqs. (29) and (30) are inequivalent, in general, when related by a Legendre transform. They can be shown, however, to be equivalent to linear order in $V_{PP}(r)$.

IV. RESULTS

A. Bulk fluid phases

In bulk, the one-body densities of both species are spatially uniform: $\rho_i(\mathbf{r}) = \mathrm{const}$. This leads to analytic expressions for the weighted densities, Eq. (7), and therefore for the excess free energy density, Eqs. (10)–(13). The integration in Eq. (6) becomes trivial and gives a factor V. Explicitly, the result is

$$\frac{\beta F_{\mathrm{exc}}(\rho_C,\rho_P)}{V} = \beta\phi_{\mathrm{HS}}(\rho_C) - \rho_P \ln\alpha_1(\rho_C) + \frac{\beta\tilde{V}_{PP}(0)}{2}\rho_P^2[1-\ln\alpha_2(\rho_C)], \tag{31}$$

where the integrated potential is $\tilde{V}_{PP}(0) = 4\pi\int dr\ r^2 V_{PP}(r) = 4\pi\epsilon\sigma_P^3/3$ and ϕ_{HS}, in the scaled-particle (Percus–Yevick compressibility) approximation, is given by

$$\beta\phi_{\mathrm{HS}} = \frac{3\eta_C[3\eta_C(2-\eta_C) - 2(1-\eta_C)^2\ln(1-\eta_C)]}{8\pi R_C^3(1-\eta_C)^2}. \tag{32}$$

In Eq. (31), the α_i, which depend solely on η_C and q, are given through

$$\ln\alpha_1 = \ln(1-\eta_C) - \sum_{m=1}^{3} C_m^{(1)}\gamma^m, \tag{33}$$

$$\ln\alpha_2 = -\tfrac{1}{8}\sum_{m=1}^{4} C_m^{(2)}\gamma^m, \tag{34}$$

where the dependence on density is through $\gamma = \eta_C/(1-\eta_C)$, and the coefficients are polynomials in the size ratio, given as $C_1^{(1)} = 3q + 3q^2 + q^3$, $C_2^{(1)} = (9q^2/2) + 3q^3$, $C_3^{(1)} = 3q^3$, and $C_1^{(2)} = 8 + 15q + 6q^2 + q^3$, $C_2^{(2)} = 15q + 24q^2 + 7q^3$, $C_3^{(2)} = 18q^2 + 15q^3$, $C_4^{(2)} = 9q^3$.

For $\beta\epsilon = 0$, our result is identical to that of free-volume theory for the AO model.[4] Central to that approach is the free volume ratio, α (defined in Sec. III D), which we find to be identical to α_1. Hence the DFT recovers free-volume theory in bulk; a discussion of relations between the two approaches can be found in Ref. 17. According to the physical meaning of α_1, we interpret α_2 as the ratio of two six-dimensional volumes, namely, the volume that is accessible to a pair of two overlapping polymer spheres and the same quantity in the absence of colloids, the latter being just $4\pi\sigma_P^3 V/3$. In Fig. 1 we plot both free volume fractions as a function of η_C for size ratios $q = 0.57$ and 1. Qualitatively, α_1 and α_2 both monotonically decrease with increasing η_C due to the excluded volume occupied by colloidal particles. Note, however, that $\alpha_2 > \alpha_1$ over the whole density range. This may be due to correlations between polymer pairs. At fixed η_C, both free-volume fractions decrease monotonically with increasing size ratio.

The total canonical free energy is given by $F/V = F_{\mathrm{exc}}/V + k_B T \Sigma_{i=C,P}\rho_i[\ln(\rho_i\Lambda_i^3) - 1]$. It is convenient to transform to the semigrand ensemble, where the polymer chemical potential instead of the system density is prescribed. The appropriate thermodynamic potential is a semigrand free energy Ω_{semi}, related to F via Legendre transform $\Omega_{\mathrm{semi}}/V = F/V - \mu_P\rho_P$, where μ_P is the chemical potential of polymers, given as

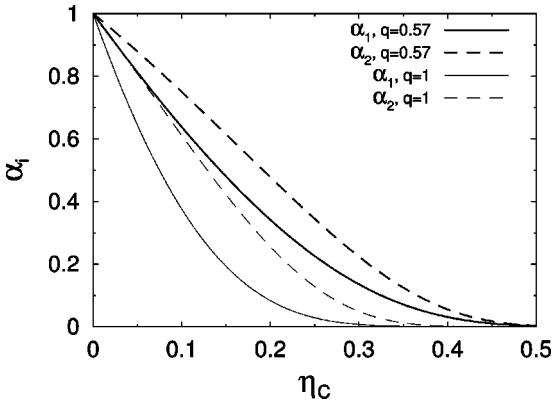

FIG. 1. Free-volume ratios of single polymers (α_1) and pairs of overlapping polymers (α_2) as a function of colloid packing fraction for polymer–colloid size ratios $q=0.57$ (top curves, thick) and $q=1$ (bottom curves, thin).

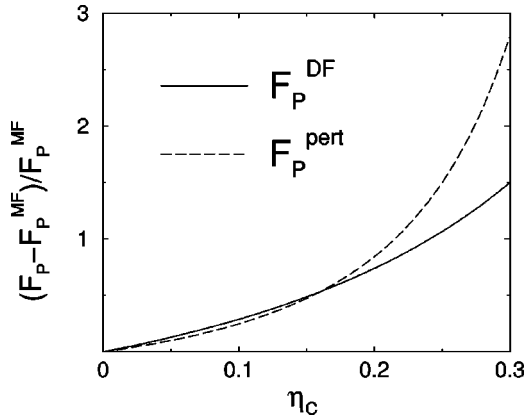

FIG. 2. Fractional excess over mean field (MF) of the free energy predicted by the density-functional (DF) and perturbative approaches [Eqs. (36) and (40)] vs colloid volume fraction η_C, for polymer–colloid size ratio $q=0.57$.

$$\beta\mu_P=\partial(\beta F/V)/\partial\rho_P$$
$$=\ln(\rho_P\Lambda_P^3)-\ln\alpha_1(\rho_C)-\beta\tilde{V}_{PP}(0)\rho_P[1-\ln\alpha_2(\rho_C)]. \tag{35}$$

Equation (35) is a transcendental equation to be solved for ρ_C once μ_P is prescribed, which is a trivial numerical task.

B. Comparison between DF and perturbative approaches

Comparing the density-functional and perturbative expressions for the bulk excess free energy [Eqs. (31) and (30), respectively], it is clear that they differ only in the interacting-polymer terms. Thus, focusing on these terms, we define the additional contribution $F_P\equiv F-F|_{\epsilon=0}$ to the free energy per volume due to polymer interactions, and find

$$\frac{F_P^{\mathrm{DF}}}{V}\equiv\frac{\tilde{V}_{PP}(0)}{2}\rho_P^2[1-\ln\alpha_2(\rho_C)] \tag{36}$$

and

$$\frac{F_P^{\mathrm{pert}}}{V}\equiv\frac{1}{2}\left(\frac{\rho_P}{\alpha_1(\rho_C)}\right)^2\int \mathrm{d}\mathbf{r}V_{PP}(r)g_{vv}(r;\rho_C). \tag{37}$$

As $r\to\infty$, two voids become uncorrelated and the void–void correlation function reduces to $g_{vv}(r)=\alpha_1^2$. Substituting this form for $g_{vv}(r)$ in Eq. (37) yields the mean-field (MF) result

$$\frac{F_P^{\mathrm{MF}}}{V}=\frac{\tilde{V}_{PP}(0)}{2}\rho_P^2, \tag{38}$$

which is independent of colloid volume fraction. Similarly, as $r\to 0$, the two voids become perfectly correlated, $g_{vv}(r)=\alpha_1$. An approximate interpolation between these two extremes was proposed in Ref. 19:

$$g_{vv}(r)=\alpha_1^2+\alpha_1(1-\alpha_1)\exp(-r/R_C). \tag{39}$$

Substituting Eq. (39) into Eq. (37) and integrating over the step-function polymer–polymer pair potential, we obtain

$$F_P^{\mathrm{pert}}=F_P^{\mathrm{MF}}\left[1+\frac{3}{4}\left(\frac{1}{\alpha_1}-1\right)q^{-3}(1-(2q^2+2q+1)e^{-2q})\right]. \tag{40}$$

We can now numerically compare the predictions of the different approximations for the interacting-polymer free energy. As the mean-field contribution is a constant (with respect to η_C), we take it as a reference and consider the fractional excess $(F_P-F_P^{\mathrm{MF}})/F_P^{\mathrm{MF}}$ as a function of η_C. Figure 2 compares the DF and perturbative results, computed from Eqs. (36) and (40). At lower colloid volume fractions ($\eta_C<0.2$) both approaches give similar results. With increasing η_C, however, there is a crossover, beyond which the approaches deviate rapidly. In fact, beyond $\eta_C\simeq 0.2$, the DF prediction increases much more gradually than the perturbative. The deviations in the free energy evident in Fig. 2 suggest a significant difference in the predicted phase behavior, which is confirmed upon explicit calculation of phase diagrams in the next section.

C. Phase diagrams

The general conditions for phase coexistence are equality of the total pressures p_{tot}, of the chemical potentials μ_i, and of the temperatures in the coexisting phases. For phase equilibrium between phases I and II,

$$p_{\mathrm{tot}}^{\mathrm{I}}=p_{\mathrm{tot}}^{\mathrm{II}}, \tag{41}$$

$$\mu_i^{\mathrm{I}}=\mu_i^{\mathrm{II}},\quad i=C,P. \tag{42}$$

These are three equations for four unknowns (two state points each characterized by two densities). Hence two-phase coexistence regions depend parametrically on one free parameter. In our case $p_{\mathrm{tot}}/k_BT=-\Phi_{\mathrm{tot}}+\Sigma_{i=C,P}\rho_i\partial\Phi_{\mathrm{tot}}/\partial\rho_i$, and $\mu_i=k_BT\partial\Phi_{\mathrm{tot}}/\partial\rho_i$, where $\phi_{\mathrm{tot}}=F/V$, yield analytical expressions. We solve the resulting sets of equations numerically, which is straightforward.

In order to compare the results from the different theoretical approaches, we consider the case of equal sizes, $q=1$, and moderately weak polymer–polymer interactions, namely $\beta\epsilon=0.25$. Our aim is to compare the fluid–fluid bin-

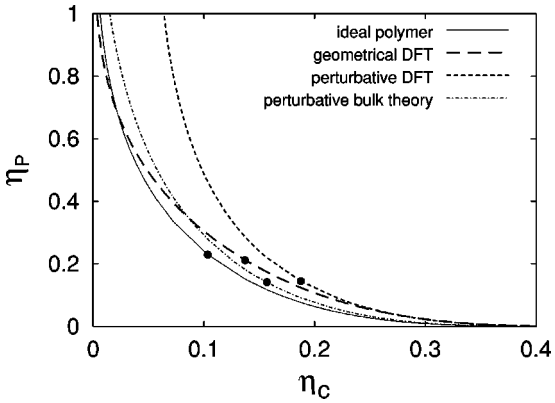

FIG. 3. Demixing phase diagram of a model colloid–polymer mixture for $q=1$ as a function of packing fractions of colloid and polymer, η_C and η_P. Shown are the theoretical binodals (lines) and critical points (dots) for ideal polymer ($\beta\epsilon=0$) as a reference case, along with the results for $\beta\epsilon=0.25$ from the geometry-based DFT, the perturbative DFT of Sec. III C, and the perturbative bulk theory of Sec. III D [Eq. (30)].

odals from the various approaches: the perturbative (Sec. III C) and geometry-based (Sec. III B) DFTs, and the perturbative bulk theory of Warren *et al.* (Sec. III D). We find that the semigrand version of the latter [Eq. (29)], when applied to our model, does not give fluid–fluid demixing for $\beta\epsilon=0.25$. Rather, the stability of demixing is restricted to a narrow range of interactions, where $\beta\epsilon$ is smaller than about 0.1. We believe that this is more a failure of the theory than of the model. As shown in Fig. 3, the binodals from the perturbative DFT and from the canonical version of the theory of Warren *et al.* [Eq. (30)] predict stabilization of the colloidal vapor phase when compared to the case of noninteracting polymers. This is at odds with the physical expectation that the polymer–polymer repulsion should *destabilize* the polymer-rich phase. In contrast, the binodal from our geometry-based DFT does capture this trend.

Stable fluid–fluid phase separation (with respect to freezing) in colloid–polymer mixtures is observed in experiments only at sufficiently large polymer-to-colloid size ratios. We consider the size ratio $q=0.57$, for which experimental data are available for poly(methyl methacrylate) (PMMA) colloid and polystyrene in *cis*-decalin.[6] Figure 4 shows the predicted phase diagrams with and without polymer interactions. For noninteracting polymers [$\beta\epsilon=0$ in Fig. 4(a)], our result is identical to that from free-volume theory. Although the predicted phase diagram may appear to capture the main experimental trends, closer inspection reveals discrepancies. Experimentally, the colloidal liquid phase contains a significant concentration of polymer, whereas the theoretical binodal for ideal polymer suggests strong dilution in polymer. In order to apply our theory to this situation, we must first prescribe the potential energy barrier.

The potential energy barrier, ϵ, can be obtained by estimating the second virial coefficient, B_2, of a pure polymer solution. For our repulsive step-function potential, B_2 is trivially related to ϵ via

$$B_2=\frac{2\pi\sigma_P^3}{3}(1-e^{-\beta\epsilon}). \tag{43}$$

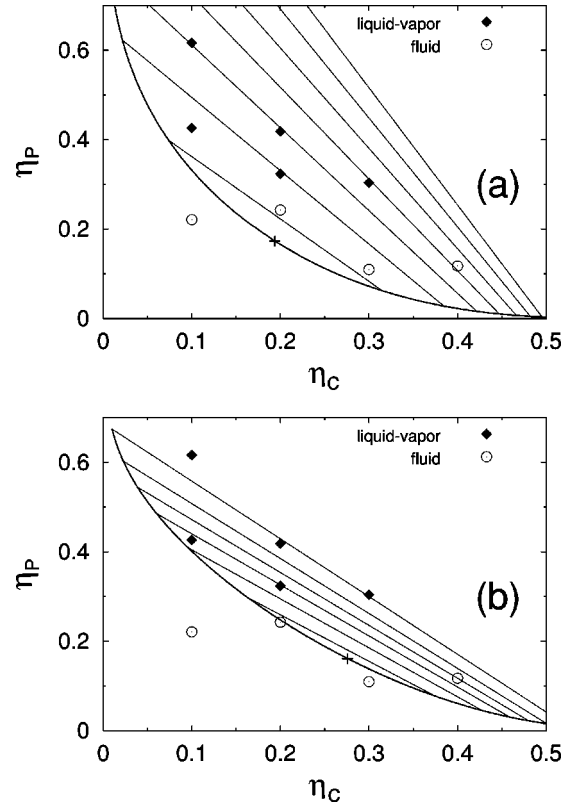

FIG. 4. Demixing phase diagram of a model colloid–polymer mixture for $q=0.57$ as a function of packing fractions of colloid and polymer, η_C and η_P. Shown are the theoretical binodal and critical point together with the experimental data of Ref. 6. (a) $\beta\epsilon=0$, equivalent to the result from free-volume theory (Ref. 4), (b) $\beta\epsilon=0.5$.

The second virial coefficient also can be expressed as[19,32]

$$\frac{B_2}{4\pi^{3/2}R_P^3}=z-4.8z^2+O(z^3), \tag{44}$$

accurate up to $z\simeq 0.1$, where z is the Fixman parameter. The Fixman parameter[32] is a measure of polymer nonideality ($z=0$ corresponding to ideal polymers) that depends on temperature, radius of gyration, and molecular mass (M). An empirical relation for z was established by Berry[32] for polystyrene in a range of hydrocarbon solvents:

$$z=0.00975\sqrt{M}\left(1-\frac{T_\theta}{T}\right), \tag{45}$$

valid over a wide range of temperatures around the theta temperature, T_θ.

Now, for the polymer–solvent system considered in Ref. 6, polystyrene in *cis*-decalin, $M=14.4\times 10^6$ and $T_\theta=12.5\,°\mathrm{C}$, while the experimental phase diagrams were measured significantly above T_θ, at $T=23\,°\mathrm{C}$. From Eq. (45), this temperature corresponds to $z=1.3$, well beyond the range of validity of Eq. (44). However, Berry[32] has measured B_2 over a considerable range of z, up to $z=5$. Thus, we can apply Eq. (44) to obtain B_2 for a small departure from ideality and then appeal to Berry's data. If we consider, for example, only a one-degree departure from T_θ, $T=13.5\,°\mathrm{C}$, then Eq. (45) gives $z=0.129$, for which Eqs. (43)

and (44) in turn yield $\beta\epsilon = 0.068$. From Berry's measurements, as z increases from 0.13 to 1.3, B_2 increases by a factor of about 5, which, from Eq. (43), corresponds roughly to $\beta\epsilon \simeq 0.5$ at $T = 23\,°\mathrm{C}$.

A second, independent, estimate of ϵ can be drawn from simulations of interacting polymer coils (in the absence of colloids).[22] At zero separation between two coils, the effective pair potential was determined to be about $(1-2)k_BT$. Hence, as a plausible value, we choose $\beta\epsilon = 0.5$. To achieve higher accuracy than provided by the linear expansion of the 0D free energy, Eq. (4), we use the cubic order expression, Eq. (5), in Eqs. (10)–(13). Figure 4 shows a comparison of the calculated theoretical binodal with the experimental data of Ref. 6.

Although the measured one-phase state point at high colloid packing fraction lies inside the theoretical two-phase region, it is obvious that our theory predicts a shift into the correct direction. We also predict that the coexisting colloidal vapor phase is more strongly diluted in colloids, as compared to the noninteracting case. All these results can be understood in terms of a free energy penalty due to polymer–polymer interactions. This primarily applies to the colloidal vapor phase. Only a small penalty arises in the colloidal liquid phase, where polymers are strongly diluted.

V. CONCLUSIONS

We have investigated a model of a colloid–polymer mixture in a good solvent, where excluded volume of monomers gives rise to a soft, penetrable repulsion between centers of masses of polymer coils. The model interpolates between the AO colloid–ideal-polymer model and binary hard spheres, through a repulsive step-function polymer–polymer interaction, whose height is a control parameter. We have derived a density-functional theory for the full crossover between both limits and have focused on the physically relevant case of weakly interacting polymers. Our theory predicts that with increasing strength of polymer–polymer interaction the coexisting colloidal liquid (vapor) phase becomes more concentrated (dilute) in polymer.

We stress that calculating bulk phase diagrams from the present theory is not more difficult than application of the original free volume theory.[4] The only additional task is to convert from the polymer fugacity to the polymer density in the system. While this can be done analytically in the free-volume theory, here we need to solve Eq. (35) numerically. In order to compare to experiment, the strength of polymer–polymer interactions must be prescribed. This quantity and the polymer-to-colloid size ratio are adjustable parameters in our model.

We have shown that a simple perturbative DFT, in which the free energy is approximated by that of an AO reference system and an additive mean-field contribution is an inappropriate approach. We believe that this failure may hold also for other binary mixtures, where an additional interaction between particles of the same species is treated as a perturbation, neglecting the presence of the other component.

A recent assessment[21] of the performance of free volume theory for the AO model in describing colloid–polymer mixtures in a good solvent (where polymers repel) found the AO model to be seriously in error, particularly for long polymer chains with a radius of gyration greater than the radius of the colloids. Here we restrict ourselves to shorter chains, where we expect an effective sphere model to be reasonable.

We emphasize that our model of polymer–polymer interactions is idealized in (at least) four ways: (i) The shape of the pair interaction is assumed to be a step function rather than a more realistic smooth, Gaussian-type function. This has a prominent effect on the structural correlation (in particular on the polymer–polymer pair distribution function). We expect, however, that predictions of the phase behavior are reasonable provided appropriate values for both model parameters, step height and range are chosen. (ii) In order to be able to derive a geometrical DFT, we set the range of the step function equal to twice the polymer radius of gyration; the latter also sets the thickness of the depletion zones around colloids. This is an ''additive'' restriction, leading to well-defined particle shapes, that can be exploited to derive the theory. In general, however, a more realistic description would be provided by a freely adjustable range of polymer–polymer interaction. This would, however, include nonadditivity as an additional complication, which we have avoided in the present study. (iii) We assume that the strength and range of the interaction are independent of the concentrations of both colloids and polymers (in general, independent of the respective one-body profiles). It is, however, known[22] that the effective polymer–polymer interaction (as obtained from simulations on the segment level) is density-dependent, although this effect appears to be quantitatively small. In principle, given some prescription of how the step height depends on the state point, this effect could be treated within the current approach. (iv) We neglect the effect of colloidal confinement on the polymer radius of gyration, and hence on the range of polymer–polymer interaction. Recently, we have modeled the influence of colloid-induced polymer compression, on demixing albeit only for the case of ideal polymer.[33] A similar model could, in principle, be applied to the case of interacting polymer.

Concerning future work, it is desirable to test our phase diagrams against simulation and more detailed experimental data for phase coexistence. It would be interesting to look at the depletion potential between colloids that is generated by the presence of nonideal polymer. The concept of integrating out degrees of freedom provides the necessary machinery, which already has been applied to limits of the present model, namely the AO[7] and HS[26] cases. Of course, more realistic polymer–polymer interactions, such as a repulsive Gaussian pair potential, are worthy of investigation. Finally, we emphasize that because our theory is intrinsically constructed to deal with inhomogeneous situations, influence of polymer interactions on the properties of interfaces and behavior near walls, such as wetting and layering phenomena[18] are problems open to investigation.

Note added. After completion of this work we became aware of a simulation study of colloid–polymer mixtures,[34] where similar phase behavior to that reported here was found.

ACKNOWLEDGMENTS

The work of one of the authors (J.M.B.) was supported by the National Science Foundation (through Grant No. CHE9800074 and the NSF Materials Research Science and Engineering Center at the University of Chicago).

[1] S. Asakura and F. Oosawa, J. Chem. Phys. **22**, 1255 (1954).
[2] A. Vrij, Pure Appl. Chem. **48**, 471 (1976).
[3] A. P. Gast, C. K. Hall, and W. B. Russell, J. Colloid Interface Sci. **96**, 251 (1983).
[4] H. N. W. Lekkerkerker, W. C. K. Poon, P. N. Pusey, A. Stroobants, and P. B. Warren, Europhys. Lett. **20**, 559 (1992).
[5] W. C. K. Poon, J. S. Selfe, M. B. Robertson, S. M. Ilett, A. D. Pririe, and P. N. Pusey, J. Phys. II **3**, 1075 (1993).
[6] S. M. Ilett, A. Orrock, W. C. K. Poon, and P. N. Pusey, Phys. Rev. E **51**, 1344 (1995).
[7] M. Dijkstra, J. M. Brader, and R. Evans, J. Phys.: Condens. Matter **11**, 10079 (1999).
[8] J. M. Brader and R. Evans, Europhys. Lett. **49**, 678 (2000).
[9] J. M. Brader, M. Dijkstra, and R. Evans, Phys. Rev. E **63**, 041405 (2001).
[10] R. Evans, in *Fundamentals of Inhomogeneous Fluids*, edited by D. Henderson (Dekker, New York, 1992), p. 85.
[11] Y. Rosenfeld, Phys. Rev. Lett. **63**, 980 (1989).
[12] Y. Rosenfeld, M. Schmidt, H. Löwen, and P. Tarazona, J. Phys.: Condens. Matter **8**, L577 (1996).
[13] Y. Rosenfeld, M. Schmidt, H. Löwen, and P. Tarazona, Phys. Rev. E **55**, 4245 (1997).
[14] P. Tarazona and Y. Rosenfeld, Phys. Rev. E **55**, R4873 (1997).
[15] P. Tarazona, Phys. Rev. Lett. **84**, 694 (2000).
[16] M. Schmidt, H. Löwen, J. M. Brader, and R. Evans, Phys. Rev. Lett. **85**, 1934 (2000).
[17] M. Schmidt, H. Löwen, J. M. Brader, and R. Evans, J. Phys.: Condens. Matter **14**, 9353 (2002).
[18] J. M. Brader, R. Evans, M. Schmidt, and H. Löwen, J. Phys.: Condens. Matter **14**, L1 (2002).
[19] P. B. Warren, S. M. Ilett, and W. C. K. Poon, Phys. Rev. E **52**, 5205 (1995).
[20] M. Fuchs and K. S. Schweizer, Europhys. Lett. **51**, 621 (2000).
[21] S. Ramakrishnan, M. Fuchs, K. S. Schweizer, and C. F. Zukoski, J. Chem. Phys. **116**, 2201 (2002).
[22] A. A. Louis, P. G. Bolhuis, J. P. Hansen, and E. J. Meijer, Phys. Rev. Lett. **85**, 2522 (2000).
[23] A. J. Archer and R. Evans, Phys. Rev. E **64**, 041501 (2001).
[24] A. J. Archer and R. Evans, J. Phys.: Condens. Matter **14**, 1131 (2002).
[25] A. A. Louis, R. Finken, and J. Hansen, Europhys. Lett. **46**, 741 (1999).
[26] M. Dijkstra, R. van Roij, and R. Evans, Phys. Rev. Lett. **81**, 2268 (1998).
[27] M. Schmidt, J. Phys.: Condens. Matter **11**, 10163 (1999).
[28] A. A. Louis, P. G. Bolhuis, and J. P. Hansen, Phys. Rev. E **62**, 7961 (2000).
[29] A. Lang, C. N. Likos, M. Watzlawek, and H. Löwen, J. Phys.: Condens. Matter **12**, 5087 (2000).
[30] C. N. Likos, A. Lang, M. Watzlawek, and H. Löwen, Phys. Rev. E **63**, 031206 (2001).
[31] H. Reiss, J. Phys. Chem. **96**, 4736 (1992).
[32] G. C. Berry, J. Chem. Phys. **44**, 1550 (1966).
[33] A. R. Denton and M. Schmidt, J. Phys.: Condens. Matter (special issue on density-functional theory) **14**, 12051 (2002).
[34] P. G. Bolhuis, A. A. Louis, and J. P. Hansen, Phys. Rev. Lett. **89**, 128302 (2002).